RSC Advances

ROYAL SOCIETY OF CHEMISTRY

www.rsc.org/advances

AFM Structural Characterization of Drinking Water Biofilm under Physiological Conditions

Authors: Stephanie L. Daniels[a,b], Jonathan G. Pressman[b], and David G. Wahman[b,*]

[a] Oak Ridge Institute for Science and Education, Oak Ridge TN, 37831, USA

[b] Water Supply and Water Resource Division, National Risk Management Research Laboratory, U.S. Environmental Protection Agency, Cincinnati, OH 45268, USA

[*] Corresponding author, mailing address: USEPA, 26 W. Martin Luther King Dr., Cincinnati, OH 45268. Phone: (513) 569-7733. Fax: (513) 487-2543. E-mail: wahman.david@epa.gov

Abstract

Due to the complexity of mixed culture drinking water biofilm, direct visual observation under in situ conditions has been challenging. In this study, atomic force microscopy (AFM) revealed the three dimensional morphology and arrangement of drinking water relevant biofilm in air and aqueous solution. Operating parameters were optimized to improve imaging of structural details for a mature biofilm in liquid. By using a soft cantilever (0.03 N/m) and slow scan rate (0.5 Hz), biofilm and the structural topography of individual bacterial cells were resolved and continuously imaged in liquid without fixation of the sample, loss of spatial resolution, or sample damage. The developed methodology will allow future in situ investigations to temporally monitor structural changes in mixed culture drinking water biofilm during disinfection treatments.

1 Introduction

Biofilm are complex microbial communities composed of various microorganisms (e.g., bacteria, fungi, protozoa, and yeast) that reversibly and/or irreversibly attach to surfaces. Microorganisms can protect themselves from the environment by producing and/or embedding into an extracellular polymeric substance (EPS) matrix comprised of proteins, lipids, and polysaccharides. The EPS influences overall biofilm behavior, impacting its adhesion, structure, and other physico-chemical properties.[1, 2] Biofilm found on interior surfaces of pipes and storage tanks and also in sediment of drinking water distribution systems have been studied and found to be a continuous source of microbial contamination, posing potential human health concerns.[1, 3-5]

In drinking water, disinfectants are used to mitigate/inactivate biofilm. The disinfectant's effectiveness to penetrate and inhibit microorganisms is influenced by the biofilm morphology (e.g., thickness, density, and porosity).[6] Therefore, there is a need to characterize the three dimensional (3D) architecture of mixed culture drinking water biofilm to understand structural-functional behaviors when exposed to disinfectant treatments. Electron and confocal microscopy have been used to elucidate the microstructure and spatial distribution of drinking water biofilm.[7-9] With electron microscopy, biological samples must be conductive, chemically fixed, and acquired under ultra-high vacuum which can introduce artifacts during imaging.[10] In confocal microscopy, sample labeling and staining can be time consuming and can also potentially produce artifacts.[11]

In contrast, atomic force microscopy (AFM) does not require elaborate sample preparation or pre-treatment, and samples can be imaged under physiological conditions, making this technique ideal for imaging biological samples.[12-14] Additionally, temporal in situ activities (e.g., growth and treatment responses) can be monitored along with localized mechanical

measurements (e.g., adhesion and detachment).[15, 16] However, most AFM studies have investigated only single species biofilm (e.g., *P. aeruginosa*,[17, 18] *E. coli*,[19, 20] and *Legionella*[21]).

Due to difficulties associated with imaging complex mixed species biofilm, only a few experiments have reported using AFM to characterize drinking water biofilm.[21-23] Specifically, Abe et al.[23] applied AFM to observe the conditioning layer of drinking water biofilm at 1-8 weeks in air and tap water. The authors acknowledged concerns of damaging the sample with the AFM cantilever and the inability to resolve individual bacteria when imaging in liquid.

When imaging soft biological materials, there are interconnected, imaging parameters that must be considered because they can influence resolution.[24-26] In Abe et al.[23], the cantilever's spring constant (k =0.1-0.5 N/m), scan rate (1 Hz), and the biofilm's young age (1-8 weeks) may have played a role in the physical disturbance of the sample and likely impacted the authors' ability to identify individual cells. When imaging biological samples in contact mode, an important parameter is the applied probe force, which can result in sample deformation or damage. Reducing the spring constant has been effective in reducing the probe force, improving resolution, and providing reproducible images.[24]

The ability to obtain microstructural details of drinking water biofilm is a prerequisite for future in situ studies for temporally monitoring drinking water biofilm exposed to disinfectants; therefore, improving AFM operating conditions are critical. The objectives of our work were to optimize imaging conditions to reduce lateral shear forces in contact mode, improve resolution, and minimize damage to an approximately three year old mixed culture drinking water biofilm in liquid. The three year growth period was to ensure a well–developed and mature biofilm, allowing our study to be made beyond the conditioning layer, which has been previously reported. [23] This is the first report to successfully demonstrate AFM's ability to characterize

topographical features and resolve individual bacteria of mixed culture drinking water biofilm without sample damage.

2 Materials and Methods

2.1 Biofilm growth conditions

Biofilm were developed in two annular reactors inoculated with water from two chloraminated drinking water distribution systems experiencing nitrification (Midwestern United States [reactor A] and southwestern United States [reactor B]) and grown on polycarbonate slides. Reactors were operated in an identical manner, both were fed granular activated carbon (Calgon F400) dechlorinated Cincinnati, Ohio, United States tap water and maintained at 25ºC. A schematic of the annular reactor setup and a detailed description of the operating conditions was previously reported by our research group and is discussed in Schrantz et al.[27] Biofilm were grown for approximately three years.

2.2 AFM characterization of drinking water biofilm

An Agilent 5500 AFM system with Pico View 1.20.1 software was used to observe morphologies of drinking water biofilm in contact mode. The polycarbonate slide containing biofilm growth was cut into approximately 0.50 cm × 0.50 cm pieces and placed in a custom designed (1.6 cm × 0.56 cm) Teflon cell for imaging. Samples imaged in air were naturally dried at room temperature while hydrated samples were imaged in 5 mM boric acid buffer solution at pH 8.

Before choosing the imaging mode, 15 cantilevers were evaluated in tap, contact, and MAC (magnetic AC) modes. Cantilevers were evaluated based on their compatibility with the Agilent system, spring constant, and the ability to image soft materials in air and liquid without

damaging the sample or compromising image resolution. Cantilever properties such as the force constant, resonance frequency, and coating are all crucial to AFM image quality and were considered. Hence, AFM cantilevers with and without coating were reviewed in both tapping and contact mode with nominal spring constants ranging from 0.03-0.77 N/m for contact mode and resonance frequencies between 4-300 kHz. Only one MAC cantilever was tested (k = 2.8 N/m). The AFM cantilevers' spring constants were taken from the manufacturers' specifications without further calibration.

For each mode, three channels were simultaneously generated: topography, amplitude, and phase (tapping mode, MAC mode) or topography, deflection, and friction (contact mode). The imaging mode and cantilever were selected based on topography image resolution. Samples were scanned at 0.50 Hz with a 256 × 256 line/pixel resolution. Collected images were processed with Gywddion software.[28]

3 Results and Discussion

For imaging fragile biological materials, the AFM cantilever's spring constant played an important role in obtaining reliable results. After evaluating various modes and cantilevers, the best images were collected in contact mode using a coated silicon cantilever CSG01, NT-MDT with a 0.03 N/m nominal spring constant. A 0V set-point and 0.5 Hz scan rate enhanced the image resolution and allowed for biofilm imaging in liquid without sample damage. With the CSG01 probe, we were able to repeatedly acquire quality images from area to area and sample to sample without comprising imaging quality or damaging the AFM cantilever. AFM images presented were imaged using the described optimized imaging conditions.

3.1 Morphology of drinking water biofilm in air

Mixed culture drinking water biofilm images in air are shown in Fig. 1. In an attempt to provide the best surface representation, scans were captured at several different sample areas. Fig. 1a is a 25×25 μm^2 image and reveals a discontinuous biofilm network with rod-like bacterial cells randomly embedded within the matrix. Darker areas in the image represent smaller or shallow features while the brighter contrast corresponds to taller features. Solid arrows in Fig. 1a highlight individual bacterial cells within the matrix. AFM is chemically blind; therefore, identifying specific biomass components is not possible, but based on previous microscopy data, the heterogeneous biomass matrix is likely composed of a combination of microbial cells surrounded by EPS.[29] After scanning several areas, the biofilm structure varied in size, thickness, and density across the sample. In the area shown in Fig. 1a, the biofilm appears to be relatively thin. Imaging in air may provide greater resolution and sharper details of the sample structure compared to liquid imaging; however, the biofilm's morphology can be altered as dehydration leads to a flattened appearance in the AFM images.[30, 31]

The 10×10 μm^2 image (Fig. 1b) is an enlargement of the rod-like shaped feature from Fig. 1a (right, solid white arrow), measuring approximately 3.6 μm in length. Surface scratches associated with the bare polycarbonate slide where no biofilm existed can also be seen (Fig. 1b, dashed white arrow). The scratches seen in Fig. 1b are a result of using 600 grit sand paper to add roughness to the slide prior to biofilm growth. Increasing the slide's surface roughness offers potential nucleation and adherence sites as well as introducing surface striations to serve as landmarks for distinguishing the bare surface from biofilm. The cursor profile in Fig. 1c represents relative changes in surface elevation along the blue line in Fig. 1b (left to right). The surface profile shows several peaks and valleys across the biofilm surface with a 0.27-μm

maximum height variation. The height measurements reflect relative variations in the surface height and not the total biofilm thickness.

3.2 Localized imaging of drinking water biofilm under physiology conditions

After successful biofilm imaging in air, the next aim was to apply the imaging parameters to characterize the sample in liquid. Fig. 2 demonstrates AFM's capability to image a mixed culture drinking water biofilm in buffer solution at pH 8. Samples shown in Fig. 2 are different samples than those in Fig. 1 but grown under identical conditions. Individual cells are randomly distributed throughout the image in Fig. 2a as shown with a white arrow. The mass inside the dotted box in Fig. 2a is a small biofilm growth. An enlargement of the area (Fig. 2b) shows some of the bacterial cells were rod shaped with smooth surfaces and others have a twisted morphology. The blue line in Fig. 2b corresponds to the cross-section shown in Fig. 2c, measuring height variation along the line from left to right. The maximum height variation is 1.3-μm as you move from areas of single cells (lower left) to a cell cluster (upper right).

Resolving individual bacterial cells within a mixed culture drinking water biofilm under physiological conditions has not been previously shown. Using a low applied force was crucial to obtaining reproducible images without sample deformation or damage to biological samples. By using a small spring constant, lateral forces between the cantilever and sample can be reduced, thus improving resolution.[24] Tapping mode is generally considered a better choice for imaging biological materials in liquids because it reduces the lateral force compared to contact mode,[32] but for the current experiments, measurements in tapping mode were not the optimal choice. Our evaluation of AFM cantilevers and imaging modes revealed that even the softest cantilevers in tapping mode were found to be intrusive on the sample and unable to produce

quality images. Magnetic AC mode provided better images compared to tapping mode; however, imaging in contact mode with the described parameters resulted in the best images. Results also showed that even though samples were grown under identical conditions, biofilm structure varied in thickness, surface coverage, and observed morphology between and within individual samples, indicating the heterogeneous nature and complexity of mixed culture drinking water biofilm.

3.3 Compilation of drinking water biofilm images

Fig. 3 demonstrates the robustness and reproducibility of the methodology to image mixed culture drinking water biofilm in air (top row) and liquid (bottom row) without compromising resolution. Air images (Fig. 3a) revealed a thick and very densely arranged biomass in the image's bottom right corner (solid arrow) along with other biofilm growth of various thickness (dashed arrow) and a few individual cells throughout. The biofilm formed a discontinuous arrangement, allowing the underlying polycarbonate surface to be visible in some locations. Long rod-shaped bacterial cells 12-30 µm in length were observed covering the image in Fig. 3b (dashed arrow). Long rods have been previous reported as cell chains that did not readily separate upon dividing.[33] Individual bacterial cells and small amorphous aggregates were also scattered throughout the image (Fig. 3b). The cells exhibited an interesting twisted configuration (Fig. 3b, solid arrow) with lengths ranging between 2.4-2.6 µm. Pelling et al.[34] observed this morphology with *Myxococcus xanthus* cells.

Fig. 3c and 3d show biofilm imaged in liquid. The samples were different from those shown in Fig. 2, although from the same reactor, validating the reproducibility of the developed method. Mixed culture drinking water biofilm samples were repeatedly imaged in liquid using

contact mode without damaging or contaminating the AFM cantilever. In Fig. 3c, the biofilm appears to be thick and densely packed in the bottom left (solid arrow). The difference between biofilm and the striated surface is clearly visible in Fig. 3c. In Fig. 3d, bacterial cells with a filament attached to the end (dashed arrow) were also resolved along with a long rod feature approximately 5.3 µm long (solid arrow).

4 Conclusions

In this study, AFM was successfully used to visualize an approximately three year old mixed culture drinking water biofilm in liquid and air. By using a cantilever with a low force spring constant (0.03 N/m) and a slow scan rate (0.5 Hz), lateral forces between the cantilever and sample were reduced and no modification to the sample surface or AFM cantilever was required. The presented AFM data demonstrated optimal imaging conditions for reproducibly capturing the microstructure of mature mixed culture biofilm beyond the conditioning layer in liquid without damaging the sample. The resolution of the biofilm's morphology in liquid was comparable to the quality obtained in air. Depending on the scanned area and the imaging environment, thin and patchy masses were observed in some areas while thicker and denser structures were visible in other locations. In addition, rod and spherical shaped bacterial cells within the biofilm were clearly distinguishable in air and liquid without resolution loss. Results from this study will allow future in situ investigations to temporally monitor structural changes in drinking water biofilm during disinfection treatments, thereby increasing our understanding of how disinfectants impact biofilm surfaces in drinking water systems.

Acknowledgements

This project was supported by an appointment to the Internship/Research Participation Program at the U.S. Environmental Protection Agency (EPA), administered by the Oak Ridge Institute for Science and Education (ORISE) through an interagency agreement between the U.S. Department of Energy and EPA. S.L. Daniels is an ORISE participant. It has been subject to the agency's peer and administrative review and has been approved for external publication. Any opinions expressed are those of the authors and do not reflect the views of the Agency; therefore, no official endorsement should be inferred. Any mention of trade names or commercial products does not constitute endorsement or recommendation for use.

References

1. Beech, I. B.; Sunner, J. A.; Hiroka, K., Microbe-surface interactions in biofouling and biocorrosion processes. *Int. Microbiol.* **2005,** *8*, 157-168.

2. Sheng, G.-P.; Yu, H.-Q.; Li, X.-Y., Extracellular polymeric substances (EPS) of microbial aggregates in biological wastewater treatment systems: A review. *Biotechnology Advances* **2010,** *28*, (6), 882-894.

3. Lu, C.; Biswas, P.; Clark, R. M., Simultaneous transport of substrates, disinfectants and microorganisms in water pipes. *Water Res.* **1995,** *29*, (3), 881-894.

4. Lehtola, M. J.; Miettinen, I. T.; Martikainen, P. J., Biofilm formation in drinking water affected by low concentrations of phosphorus. *Can. J. Microbiol.* **2002,** *48*, (6), 494-499.

5. Keinänen, M. M.; Korhonen, L. K.; Martikainen, P. J.; Vartiainen, T.; Miettinen, I. T.; Lehtola, M. J.; Nenonen, K.; Pajunen, H.; Kontro, M. H., Gas chromatographic–mass spectrometric detection of 2- and 3-hydroxy fatty acids as methyl esters from soil, sediment and biofilm. *J. Chromatogr. B* **2003,** *783*, (2), 443-451.

6. Lee, W. H., Wahman, D.G., Bishop, P.L., Pressman, J.G., Free chlorine and monochloramine application to nitrifying biofilm: Comparison of biofilm penetration, activity, and viability. *Environmental Science & Technology* **2011,** *45*, 1412-1419.

7. Sun, W. J.; Liu, W. J., Impact of the ultraviolet disinfection process on biofilm control in a model drinking water distribution system. *Environ. Eng. Sci.* **2009,** *26*, (4), 809-816.

8. Hong, P. Y.; Hwang, C. C.; Ling, F. Q.; Andersen, G. L.; LeChevallier, M. W.; Liu, W. T., Pyrosequencing analysis of bacterial biofilm communities in water meters of a drinking water distribution system. *Appl. Environ. Microb.* **2010,** *76*, (16), 5631-5635.

9. Janjaroen, D.; Ling, F.; Monroy, G.; Derlon, N.; Mogenroth, E.; Boppart, S. A.; Liu, W.-T.; Nguyen, T. H., Roles of ionic strength and biofilm roughness on adhesion kinetics of

Escherichia coli onto groundwater biofilm grown on PVC surfaces. *Water Res.* **2013,** *47*, (7), 2531-2542.

10. Lazarova, V.; Manem, J., Biofilm characterization and activity analysis in water and wastewater treatment. *Water Res.* **1995,** *29*, (10), 2227-2245.

11. de Carvalho, C.; da Fonseca, M. M. R., Assessment of three-dimensional biofilm structure using an optical microscope. *Biotechniques* **2007,** *42*, (5), 616-620.

12. Radmacher, M., Tillmann, R.W., Fritz, M., Gaub, H. E., From molecules to cells: Imaging soft samples with the atomic force microscope. *Science* **1992,** *257*, 1900-1903.

13. Ahimou, F.; Semmens, M. J.; Novak, P. J.; Haugstad, G., Biofilm cohesiveness measurement using a novel atomic force microscopy methodology. *Applied and Environmental Microbiology* **2007,** *73*, (9), 2897-904.

14. Webb, H. K., Truoug, V.H., Hasan, J., Crawford, R.J., Ivanova, E.P.,, Physico-mechanical characterisation of cells using atomic force microscopy-Current research and methodologies. *Journal of Microbiological Methods* **2011,** *86*, 131-139.

15. Bowen, R. W. L. R. W. W. C. J., Applications of atomic force microscopy to the study of micromechanical properties of biological materials *Biotechnology Letters* **2000,** *22*, 893-903.

16. Dufrêne, Y. F., Atomic Force Microscopy in Microbiology: New Structural and Functional Insights into the Microbial Cell Surface. *mBio* **2014,** *5*, (4).

17. Touhami, A.; Jericho, M. H.; Boyd, J. M.; Beveridge, T. J., Nanoscale Characterization and Determination of Adhesion Forces of Pseudomonas aeruginosa Pili by Using Atomic Force Microscopy. *Journal of Bacteriology* **2006,** *188*, (2), 370-7.

18. DeQueiroz, G. A.; Day, D. F., Antimicrobial activity and effectiveness of a combination of sodium hypochlorite and hydrogen peroxide in killing and removing Pseudomonas aeruginosa biofilms from surfaces. *Journal of Applied Microbiology* **2007,** *103*, (4), 794-802.

19. Bolshakova, A. V.; Kiselyova, O. I.; Filonov, A. S.; Frolova, O. Y.; Lyubchenko, Y. L.; Yaminsky, I. V., Comparative studies of bacteria with an atomic force microscopy operating in different modes. *Ultramicroscopy* **2001,** *86*, (1–2), 121-128.

20. Lim, J. L., K. M.; Kim, S. H.; Nam, S.W.; Oh, Y.J.; Yun,H.S.; Jo, W.; Oh, S.; Kim, S.H.; Park, S., Nanoscale Characterization of Escherichia Coli Biofilm Formed under Laminar Flow Using Atomic Force Microscopy (AFM) and Scanning Electron Microscopy (SEM). *Bulletin Korean Chemistry Society* **2008,** *29*, (11), 2114-2118.

21. Gamby, J., Pailleret, A., Clodic, C.R., Pradier, C.M., Tribollet, B., In site detection and characterization of potable water biofilms on materials by microscopic, spectroscopic and electrochemistry methods. *Electrochimica Acta* **2008,** *54*, 66-73.

22. Abe, Y.; Skali-Lami, S.; Block, J.-C.; Francius, G., Cohesiveness and hydrodynamic properties of young drinking water biofilms. *Water Res* **2012,** *46*, (4), 1155-1166.

23. Abe, Y., Polyakov, P., Skali-Lami, S., Francius, G., Elasticity and physico-chemical properties during drinking water biofilm formation. *Biofouling* **2011,** *27*, (2), 739-750.

24. Shao, Z.; Mou, J.; Czajkowsky, D. M.; Yang, J.; Yuan, J.-Y., Biological atomic force microscopy: what is achieved and what is needed. *Adv. Phys.* **1996,** *45*, (1), 1-86.

25. Gan, Y., Atomic and subnanometer resolution in ambient condition by atomic force microscopy. *Surf. Sci. Rep.* **2009,** *64*, (3), 99-121.

26. Méndez-Méndeza, J. V.; Alonso-Rasgado, M. T.; Correia Faria, E.; Flores-Johnson, E. A.; Snook, R. D., Numerical study of the hydrodynamic drag force in atomic force microscopy measurements undertaken in fluids. *Micron* **2014,** *66*, 37-46.

27. Schrantz, K. A.; Pressman, J. G.; Wahman, D. G., Simulated distribution nitrification: Nitrification index evaluation and viable AOB. *JAWWA* **2013,** *105*, (5), 55-56.

28. Neˇcas, D.; Klapetek, P., Gwyddion: an open-source software for SPM data analysis. *Cent. Eur. J. Phys.* **2012,** *10*, (1), 181–188.

29. Flemming, H. C., Biofouling in water systems – cases, causes and countermeasures. *Appl Microbiol Biotechnol* **2002,** *59*, (6), 629-640.

30. Volle, C. B.; Ferguson, M. A.; Aidala, K. E.; Spain, E. M.; Núñez, M. E., Spring constants and adhesive properties of native bacterial biofilm cells measured by atomic force microscopy. *Colloids and Surfaces B: Biointerfaces* **2008,** *67*, (1), 32-40.

31. Wright, C. J. S., M.K.; Powell, L.C.; Armstrong, I., Application of AFM from Microbial Cell to Biofilm. *Scanning* **2010,** *32*, 134-149.

32. Dorobantu, L. S.; Goss, G. G.; Burrell, R. E., Atomic force microscopy: A nanoscopic view of microbial cell surfaces. *Micron* **2012,** *43*, (12), 1312-1322.

33. Braga, P. C.; Ricci, D., Differences in the susceptibility of *Streptococcus pyogenes* to rokitamycin and erythromycin A revealed by morphostructural atomic force microscopy. *J. Antimicrob. Chemother.* **2002,** *50*, (4), 457-460.

34. Pelling, A. E.; Li, Y.; Shi, W.; Gimzewski, J. K., Nanoscale visualization and characterization of Myxococcus xanthus cells with atomic force microscopy. *Proceedings of the National Academy of Sciences of the United States of America* **2005,** *102*, (18), 6484-9.

305 **Fig. 1.** AFM images of mixed culture biofilm grown on polycarbonate slides. AFM data was
306 acquired in air with contact mode. (a) 25 × 25 μm^2 image size, (b) 10 × 10 μm^2 image size, and
307 (c) height profile corresponding to blue line in (b).

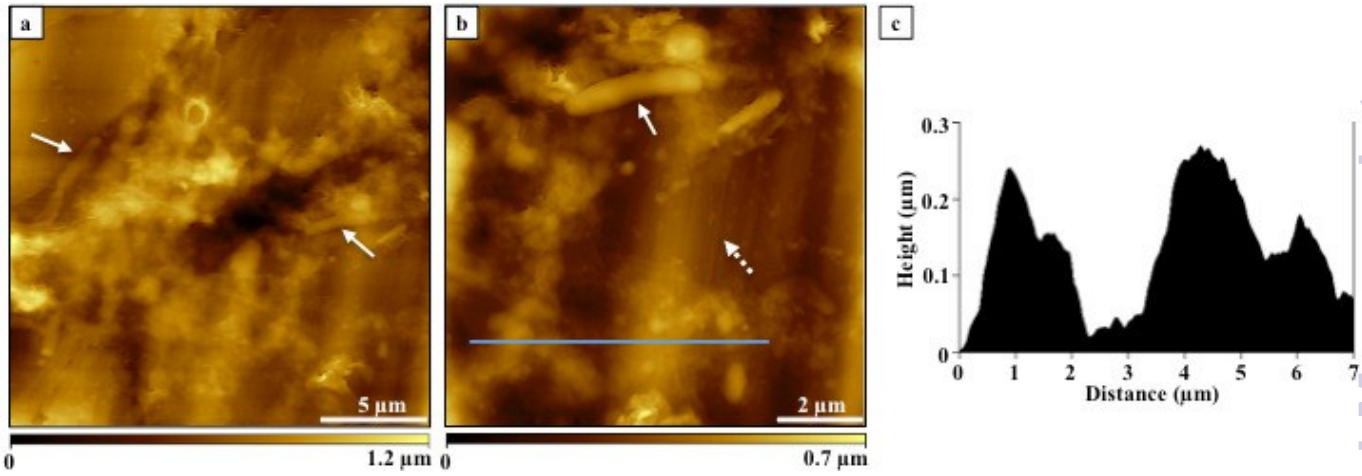

308

309

310 **Fig. 2.** Mixed culture drinking water biofilm observed in 5 mM boric acid buffer solution at pH
311 8 with contact mode. (a) 70×70 μm^2 image size, (b) 35×35 μm^2 image size, and (c) height profile
312 corresponding to the area underneath the blue line in image (b).

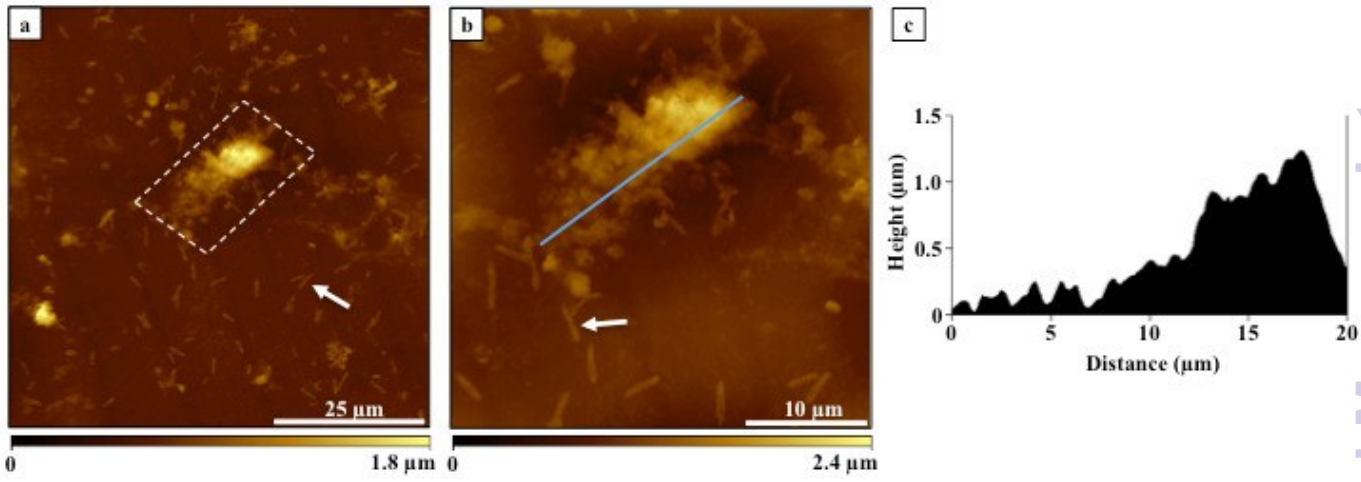

313

314

315 **Fig. 3.** AFM image gallery of various morphologies found in a mixed culture drinking water
316 biofilm. Top row was acquired in air with image sizes of (a) 45×45 μm^2 and (b) 30×30 μm^2.
317 Bottom row was acquired in 5 mM boric acid buffer solution at pH 8 with image sizes of (c)
318 80×80 μm^2 and (d) 10×10 μm^2.

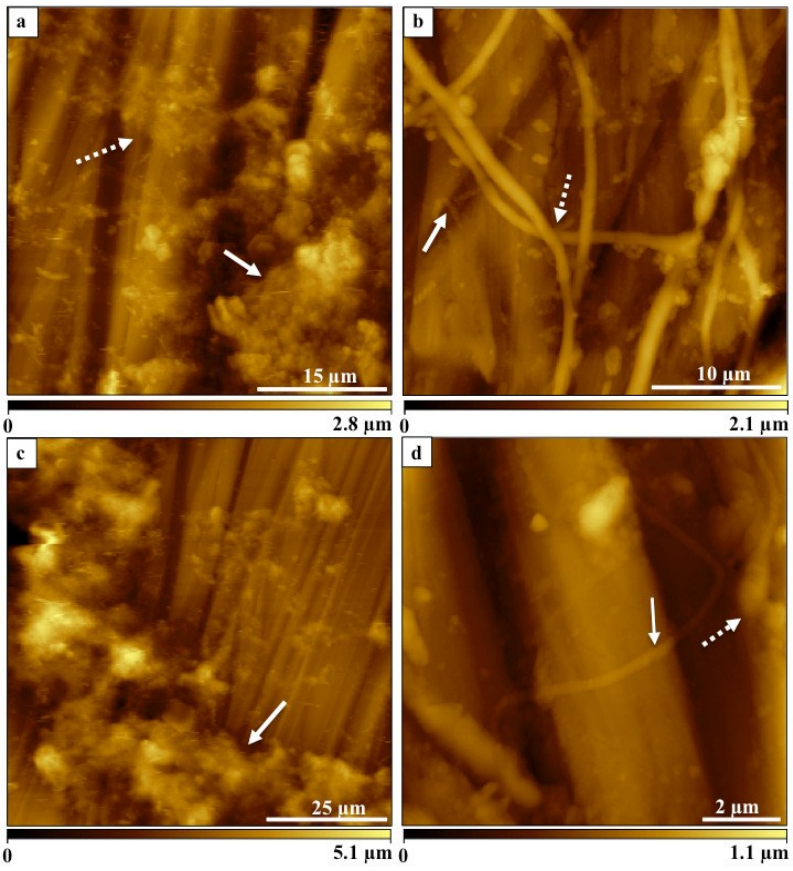

319

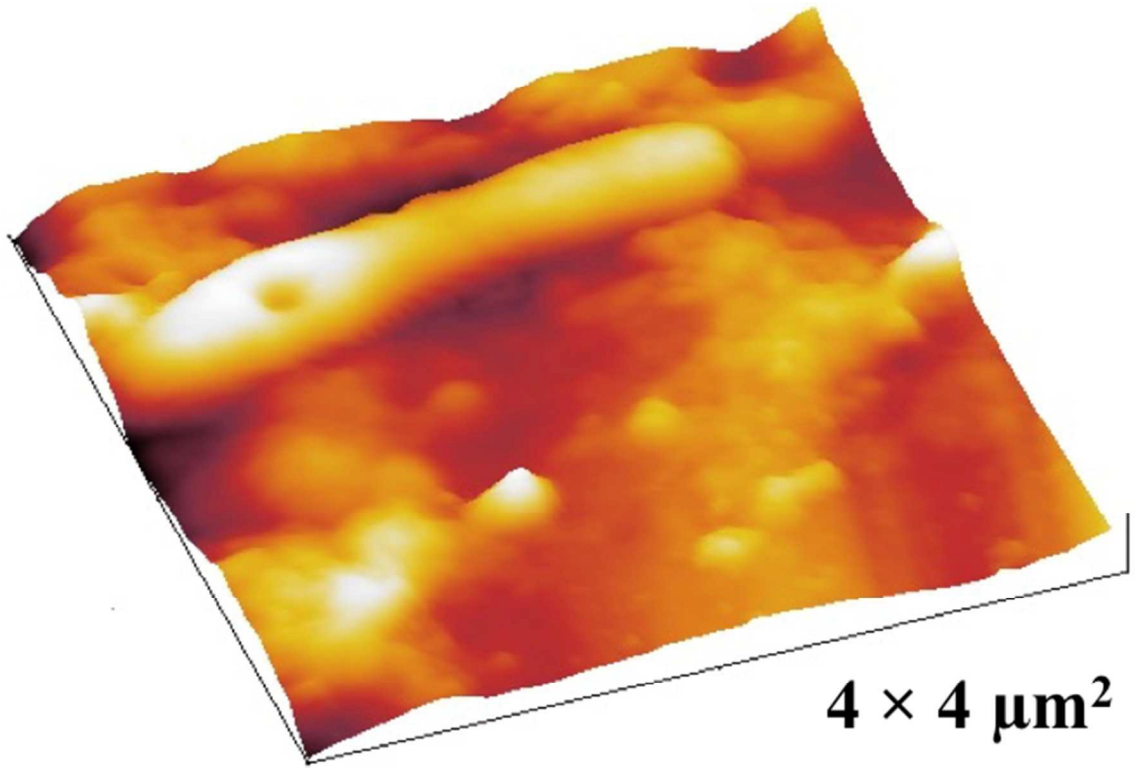

Insights into the complex morphology of multi-species drinking water biofilm using atomic force microscopy (AFM)